Fingertip-based Feature Analysis for the Push and Stroke Manipulation of Elastic Objects

Megumi Nakao, *Member, IEEE,* Masayuki Senoo, and Tetsuya Matsuda, *Member, IEEE*

Abstract—In this study, to quantitatively understand finger operations used to manipulate elastic objects, we explore robust fingertip-based feature descriptors that are invariant to operator, finger position, and target object. To measure the tactile information generated when an object is directly touched by a fingertip, we used a wearable system that enables the simultaneous measurement of fingertip position and strain without inhibiting the operator's sense of touch. This paper focuses on the quantitative classification of the push and stroke operations of a single finger, and conducted user experiments to obtain time-series fingertip position and strain from 10 subjects touching nine types of elastic objects. The recognition rate was investigated by binary classification using a support vector machine and cross validation. The results show that the two-dimensional features obtained from fingertip position and strain within a 0.9-s time frame can stably recognize push and stroke operations on elastic bodies of different shapes, stiffnesses, and thicknesses at a higher recognition rate.

Index Terms—Fingertip-based recognition, haptic interaction analysis, finger manipulation, wearable sensor

1 Introduction

HUMAN beings perceive the world through their fingers, and through delicate and complex finger movements, skillfully manipulate objects of a wide variety of shapes and materials. The tactile information generated between fingers and an object plays a major role in determining the appropriate finger operation and is an important indicator for quantitatively understanding the finger operation mechanism [1], [2], [3], [4], [5]. In the medical field, there have been attempts to develop technical training and educational systems for finger operations that require advanced levels of knowledge and experience such as the use of surgical tools for palpation and endoscopic surgery [6], [7], [8], [9]. In robotics, sensory information gained by humans during finger operations has been measured and analyzed [10], [11], [12], [13], [14], [15]. The objective of such research is to advance the control and design of manipulators [16], [17], [18] capable of performing actions similar to or even more accurate than human finger operations.

Tactile information can be sensed by a body part directly touching an object. Compared with kinematics or hand/finger motion [19], [20], [21], [22], which can be captured using optical tracking or magnetic sensors, measuring, analyzing, and sharing natural finger manipulation using haptic feedback is not simple. Virtual reality (VR) simulators have achieved haptic interaction with a virtual model using a force feedback device. The ability to generate artificial haptic feedback (e.g., tactile illusion) enables the investigation of human perception [2], [23], decision making [24], and mechanisms of dexterous manipulation [25], [26]. In the medical field, there have been efforts [7], [8], [27] to develop VR simulation systems wherein organ manipulation via palpation and surgical tools can be experienced in simulation as surgical training for doctors. VR systems in which multiple people can simultaneously touch the same location of a virtual object enables tactile information to be shared with other people [28]. In these studies, by constructing a virtual object model that suitably reflects the three-dimensional (3D) form and mechanical properties of the target object, it becomes possible to measure and quantitatively analyze simulated finger operations. However, there are differences between artificial reality and the real world. Because it is not easy to accurately reproduce the texture and elastic properties of real objects, the divergence between vision and sense of touch during finger operations is not negligible.

Many studies have attempted to directly measure hand operations associated with actual objects to better share tactile information. By measuring the force generated along with the 3D position and posture of the fingertips when an actual object or tool is touched, tactile information can be quantitatively measured [24], [29]. However, previous studies using such methods had to embed measurement sensors in the object [30] or attach sensors to the palms or fingertips [21], [31], [32], [33], [34]. Although it is possible to directly embed sensors in the object, the measurable area is limited and the object's force features may be affected by the sensors. In the latter method, while the measurable area is not limited, the sensor attached to the palm or fingertips may interfere with finger sensations during operations [34], [35]. Measuring the tactile information obtained when an actual object is touched in an environment in which natural finger operations are possible remains a challenge, and the measurement and analysis of finger operations on actual objects are still limited.

In this study, our aim is to quantitatively examine finger operations that target actual objects. We hence construct a finger operation measurement system that does not inhibit fingertip sensation. We furthermore conduct a quantitative analysis of multidimensional features in experimentally

• *M. Nakao, M. Senoo and T. Matsuda are with Graduate School of Informatics, Kyoto University, Yoshida-Honmachi, Kyoto, Sakyo, 606-8501, JAPAN.*
E-mail: megumi@i.kyoto-u.ac.jp

Manuscript received August 1, 2016; revised August 1, 2017.

measured finger operation data. According to the previous literature [36], hand movement can be categorized into eight types of motion patterns: lateral motion, pressure, static contact, unsupported holding, enclosure, contour following, function test, and part motion test. This paper focuses on fingertip-based classification of the two fundamental actions, lateral motion and pressure, on a fixed elastic object. We assume that one possible application of this feature selection is a quantitative understanding of finger operation by medical experts. Push and stroke operations with one finger are a basic, essential skill for medical palpation procedures [7], [8]. Medical experts use different finger operations depending on the location and the shape of the target organs. The relationship between fingerpad state and decision-making would contribute to understanding the skills of fingers, and will be useful for developing training scenarios or dexterous robotic system design. Another application of finger operation recognition is to use the finger-attached wearable sensor as novel tangible interface for computers. A variety of input styles using real-world objects has been considered [37], [38]. Integrating wearable sensors and finger operation recognition will bring us one step closer to such ubiquitous input environments.

For the analysis of dexterous manipulation across the human and robotic domains, Bullock et al. presented a hand-centric classification scheme [14]. Makino et al. [39] proposed a life log system to record fingertip information in our daily lives. However, to the best of our knowledge, few studies have focused on the fingertip-centric recognition of haptic interaction with real-world elastic objects. As a first step toward a fingertip-based classification scheme, this study focuses on push and stroke operations with relatively detailed motion on a small region of an elastic object. To reduce the complexity of classification, the overall hand motion including wrist and palm motion was considered to be out of scope of this paper. In spite of this simplification, a variety of applications can be considered because push and stroke operations are recognized by recent touch interfaces. Because similar fingertip-based input styles are used for most desktop tasks, real-world deformable objects with any shape could become a touch screen [37], [40], [41] if wearable fingertip sensors are used. Push and stroke operations are also used to recognize stiffness, texture, and elasticity of the target object, not to move or change its orientation. Palpation by surgeons or medical practitioners is a clinically practical example and is used to localize tumors [13], [27] for diagnosis or decision-making during surgery [7].

Based on these motivations, if the intended touch interaction on fixed objects with a fingerpad is possible without obstructing the sense of touch, we consider that "natural" finger operation has been achieved in this study. To identify and understand push and stroke interaction with an index finger, we focus on measuring the fingertip while touching different types of elastic objects. Specifically, our interest is the exploration of low-dimensional robust descriptors that are invariant to finger position, target shape, and physical properties. The direction of this study, therefore, is to address the following issues by quantitatively analyzing single-finger push and stroke operations:

- Measurement of natural finger operations using a single finger and actual objects
- Exploration of robust feature descriptors that are invariant to operator, finger position, and target object
- Quantitative classification of push and stroke operations for actual objects with different shapes, materials, and stiffnesses

To measure natural finger operations used to touch elastic objects, we constructed an experimental system in which fingertip strain and 3D fingertip position could be simultaneously measured without inhibiting fingertip sensation. Experiments were conducted with 10 subjects using various types of elastic bodies, and the multidimensional feature values of push and stroke operations were investigated. Based on the determined feature sets, operations were classified using a support vector machine (SVM) and cross validation. The performance of the calculated decision boundaries to classify push and stroke operations was evaluated.

2 Materials and Methods

2.1 Measurement system

To analyze natural human finger operations, we focused on the simultaneous measurement of 3D position and fingertip strain, key factors that affect the sense of touch when the operator touches actual objects. For the finger operation measurement, therefore, we reproduced the following measurement environment:

- No object or physical restrictions on the movement of the operator or fingertip operation
- Simultaneous measurement of fingertip strain and position without depending on the operator's posture
- No device attached to the fingerpad section and no obstruction of the operator's sense of touch on the fingerpad.

To realize measurements satisfying these conditions, we designed a fingertip position and strain measurement system, as shown in Figure 1a. For strain, we used a HapLog (Tec Gihan Co., Ltd., JAPAN) with 16-bit resolution to measure the deformity of the fingerpad in the horizontal direction. The HapLog device does not cover the fingerpad; thus, it does not obstruct the operator's fingertip sensation or sense of touch [35], [42]. To measure fingertip position, we used a 3D Guidance MedSAFE sensor (Ascension Technology Corporation, USA), a compact magnetic position sensor that can detect 3D positions with a resolution of 0.5 mm and a root-mean-square error of 1.4 mm [34]. We considered the use of an on-board accelerometer for the HapLog, but we found there was considerable noise in the position and velocity computation using the measured acceleration values when small finger manipulations were applied to elastic objects. Because we targeted millimeter-order finger operations, an accurate positional sensor with sufficient spatial resolution is suitable for the purposes of these experiments. We also considered other optical and mechanical measurements; however, optical systems tend to be influenced by occlusion of the object or adjacent fingers when the object is touched by the fingertip. Finger

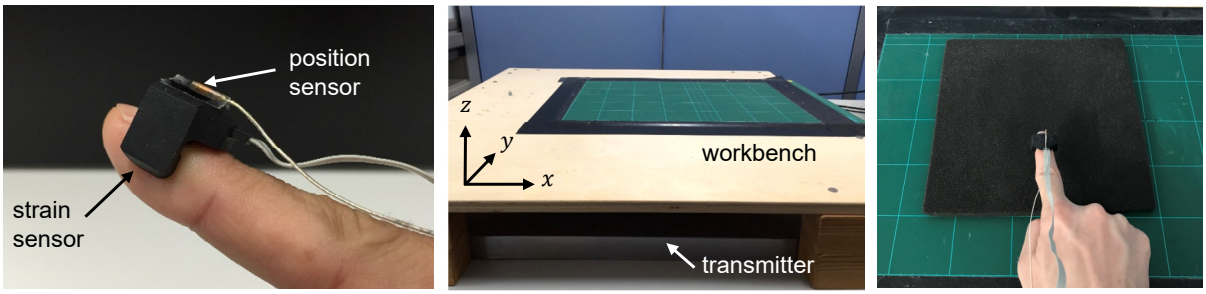

Fig. 1. Measurement system and workspace for capturing finger operation: a) wearable position/strain sensor designed to capture natural finger operation without obstructing the sense of touch, b) workbench with the transmitter for the magnetic position sensor, and c) push operation test using a wooden cube.

movement is often limited in other mechanical systems. Thus, for this study, we adopted a magnetic motion capture system, which is not affected by occlusion and does not limit finger movement.

By mounting the magnetic position sensor on top of the strain sensor, strain and fingertip position can be measured without obstructing the operator's finger movement or sense of touch. We constructed a workbench to affix the transmitters needed to generate the magnetic fields of the magnetic position sensor. The relative positions of the transmitter and workbench as well as the workspace coordinates used during the experiments are shown in Figure 1b. Using software we created for synchronous sampling, the 3D fingertip position $\mathbf{p}(t) = (x(t), y(t), z(t))$ and strain value $\epsilon(t)$ were simultaneously recorded at sampling intervals of 30 ms. Figure 1c shows an instance wherein the measurement sensor is attached to the index finger of the experimenter while the top of a wooden cube is pushed. Fingertip velocity $v(t)$ was calculated from $\mathbf{p}(t)$, and normalized strain $\epsilon_n(t)$ was calculated based on

$$\epsilon_n(t) = 100 \times (\epsilon(t) - \epsilon_0)/(\epsilon_1 - \epsilon_0) \quad (1)$$

where ϵ_0 is the threshold value used to detect physical contact between the finger and the object, and ϵ_1 is the reference value calibrated per an operator when a 1000-g push operation is applied to an electronic scale with the index finger. We note that the fingerpad deforms because of the bending of joints and tension on the fingertips even when the operator does not directly touch an object. Furthermore, the values received from the strain sensors differ greatly depending on the shape and size of the operator's fingers. Because this study aimed to analyze features of finger operation when a finger manipulates an object, contact between the finger and object was detected. It was also necessary to reduce the impact on the measurement data caused by the difference in finger shape between operators. Thus, a 10-s calibration procedure was performed in advance and the fingertip strain when performing translation, rotation, and bending finger operations in free space (i.e., a non-touching state) was measured. The start and end points of an operation on the actual object were determined using $\epsilon_0 = \mu + 3\sigma$, where μ is the average value and σ is the standard deviation of the strain obtained from the calibration procedure.

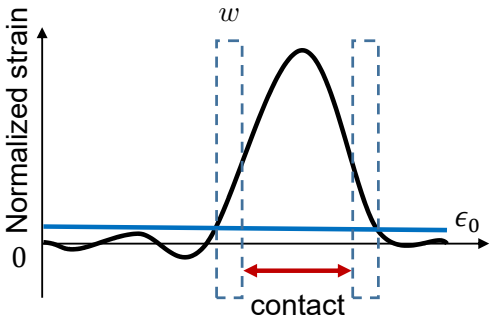

Fig. 2. Contact detection using normalized strain data. Contact is determined when the normalized strain values of the past w samples are all positive.

An example of the transition in strain values $\epsilon(t)$ when starting a push operation on an elastic object is shown in Fig. 2. Using window width parameter w, a contact state is determined when the normalized strain values of the past w samples are all positive, which is defined by

$$\epsilon_n(t - k\Delta t) > 0 \quad (\forall k \in \mathbb{N}, 0 \leq k \leq w - 1) \quad (2)$$

The measured data in the contact state are the target of the feature value calculation. As the sampling interval Δt is 30 ms in this study, in the case of $w = 10$, for instance, 10 samples in the 300 ms are used for contact detection and for feature value calculation.

2.2 Elastic objects

To measure finger operations used to manipulate multiple elastic materials, the elastic bodies with different shapes, materials, and stiffnesses shown in Figure 3 were used as operation targets. Three types of low-resilience urethane (10-, 20- and 30-mm-thick) and four types of gel (hard cuboid, soft cuboid, soft hemispherical, and soft triangular prism) were prepared. To quantitatively confirm the stiffness of these elastic bodies, we measured Young's modulus using the YAWASA stiffness measurement device (Tec Gihan Co., Ltd., JAPAN). Young's modulus was 47.48 kPa, 79.36 kPa, and 285.2 kPa for low-resilience urethane, soft gel, and hard gel, respectively. Considering that that Young's modulus for the silicone rubber and wooden materials was approximately 1×10^4 kPa and 1×10^7 kPa, respectively, we

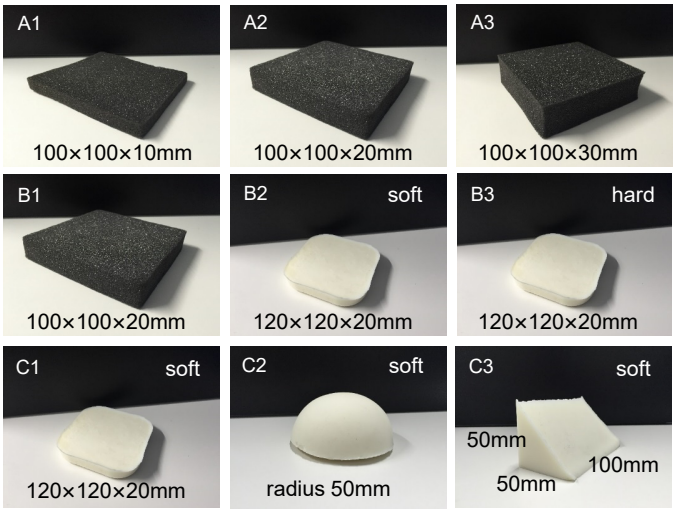

Fig. 3. Elastic objects with different shapes, materials, and stiffnesses. Three groups of elastic objects with A) different thicknesses, B) different stiffnesses, and C) different shapes were prepared for the experiments.

can see that these three types of elastic bodies are all soft materials. In the experiments, nine elastic objects: A) three with different thicknesses, B) three with different stiffnesses, and C) three with different shapes were used. Note that the bottom surface of the target object was fixed to the workbench during the measurement process.

2.3 Multidimensional Feature values

One of the challenges in this study is to robustly identify natural operations on various types of elastic objects using the strain and velocity of a fingertip. Figure 4 shows the typical time changes of normalized strain $\varepsilon_n(t) \in \mathbb{R}$ and velocity $v(t) \in \mathbb{R}$ for a fingertip performing push and stroke operations. There are large differences between the push and stroke operations in Fig. 4a. In the push operation, the fingers and object come into contact, whereas this contact transitions with a value close to 0 in time band $v(t)$. When $\varepsilon_n(t)$ is large during the stroke operation, we can confirm from the $v(t)$ behavior that the finger movement occurs because of the stroke operation in the time frame over which the finger touches the object. Time variations for $\varepsilon_n(t)$ and $v(t)$ for the push and stroke operations on the hemispheric gel are shown in Fig. 4b. Relative to Fig. 4a, little difference is observed, and interestingly, the magnitude of the normalized strain during the push operation is relatively smaller than that during the stroke operation. Furthermore, if we compare the measured data obtained from the stroke operation in Fig. 4a and the data from the push operation in Fig. 4b, no major difference can be found. These results come from the natural variation of a subject's finger operations when touching different elastic objects. Our aim in this study was to investigate whether quantitative classification of the push and stroke operations from these measured data is possible.

To quantitatively analyze natural finger operations, we focused on robust feature values that are invariant to fingertip position, orientation, and operation target. In this study, the following four candidate feature values were selected and calculated from the time-series measured data.

- Moving average of velocity: $v_a(t, w)$
- Standard deviation of velocity: $v_\sigma(t, w)$
- Moving average of normalized strain: $\epsilon_a(t, w)$
- Standard deviation of normalized strain: $\epsilon_\sigma(t, w)$

where w is the width of the time-frame window. Obviously, it is difficult to classify push and stroke operations from measurement values taken at a single point in time. Multidimensional feature values that can be extracted from the measured data over time frames of width w in the contact state were used. The selected feature values were calculated using the following equations:

$$v_a(t, w) = \sum_{k=0}^{w-1} \frac{v(t - k\Delta t)}{w} \tag{3}$$

$$v_\sigma(t, w) = \sqrt{\sum_{k=0}^{w-1} \frac{\{v(t - k\Delta t) - v_a(t, w)\}^2}{w}} \tag{4}$$

$$\varepsilon_a(t, w) = \sum_{k=0}^{w-1} \frac{\varepsilon(t - k\Delta t)}{w} \tag{5}$$

$$\varepsilon_\sigma(t, w) = \sqrt{\sum_{k=0}^{w-1} \frac{\{\varepsilon(t - k\Delta t) - \varepsilon_a(t, w)\}^2}{w}} \tag{6}$$

The multidimensional strain and velocity information on a fingertip within specific time frames should efficiently evaluate finger operations. Specifically, we hypothesized that a human's push and stroke operations can be classified by low-dimensional features of the fingerpad information. These values are invariant to finger position, target shape, and physical properties. To explore low-dimensional, robust feature sets and their classification performance, we designed user experiments to measure natural finger operations on elastic objects. As the best window parameter w for identifying push and stroke operations for a variety of objects is not evident, w was selected based on a statistical analysis, i.e., the classification performance for the measured data obtained from the experiments.

3 Experiments and Results

3.1 Experimental procedures

Ten healthy subjects (1/10 females, all right-handed, 23 ± 2 years old, mean$\pm$ SD) participated in the experiment. In accordance with the ethical guidelines of Kyoto University for research involving human subjects, all participants gave informed consent to participate in the study.

In the experiment, each participant wore the position/strain sensor on his/her index finger and executed push and stroke operations on the elastic objects. The subjects freely manipulated the objects in one operation, which was repeated five times while changing the method of touch. Three-dimensional fingertip position $\mathbf{p}(t) \in \mathbb{R}^3$ and strain $\epsilon(t) \in \mathbb{R}$ were measured using the measurement system. Nine types of elastic objects shown in Fig 3 were used to investigate the robustness of the proposed feature values. The initial device setup, a short practice, calibration, and measurements were performed according to the following procedures.

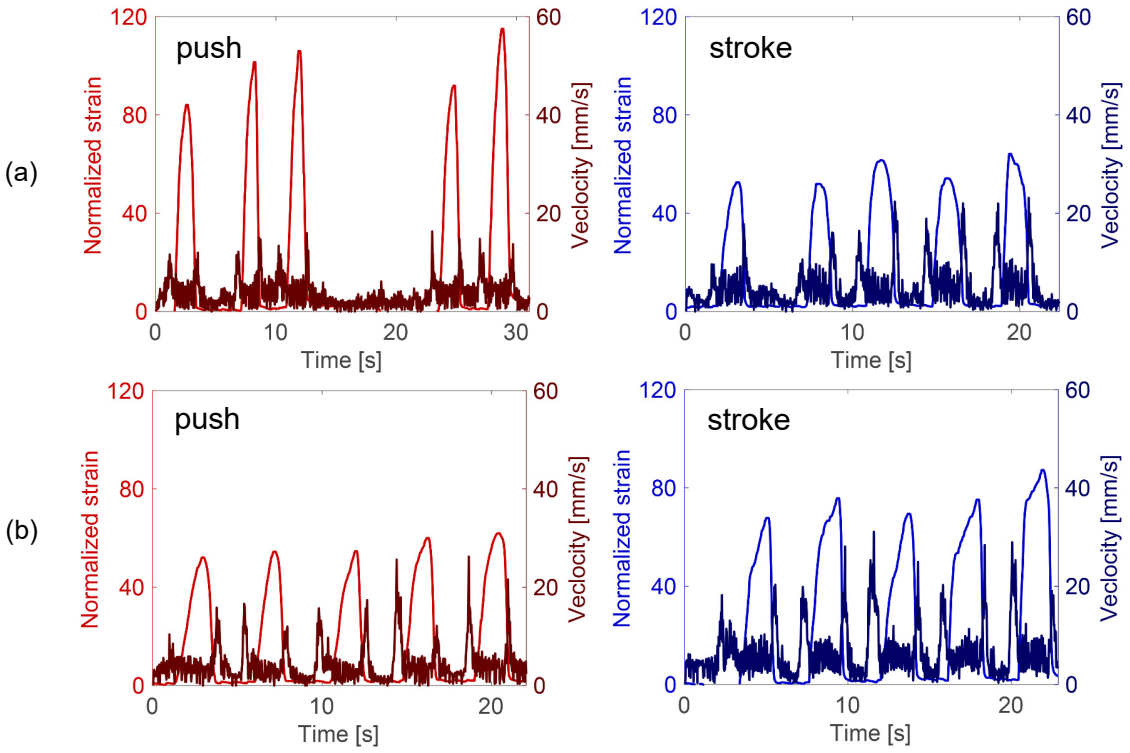

Fig. 4. Typical measured strain and velocity of a fingertip over time when touching (a) cuboid low-resilience urethane and (b) a hemispheric gel five times.

- The operator sat in a chair facing the elastic object placed on the workbench. The height of the chair was adjusted so that the operator could freely push/stroke the surface of the elastic objects.
- The operator attached the measurement sensor to the index finger on the right hand.
- For hand operations with the measurement sensor attached, a practice time of 10 s was allowed for the first target elastic body to confirm that the fingertip senses of the operator were not obstructed.
- To determine contact detection threshold ϵ_0, fingertip strain was measured for 10 s when executing parallel finger pointing and rotation operations.
- To normalize the strain values, strain value ϵ_1 was measured for a 1000-g push operation with the index finger using an electronic scale.
- Fingertip position $\mathbf{p}(t)$ and strain $\epsilon(t)$ for the push and stroke operations for the surface of each elastic body were measured five times.

When conducting the push and stroke operations, each operator was instructed to change the contact position, finger pressure, fingertip movement direction, and amount of fingertip movement on the surface of the elastic body. Each operator was also instructed to perform the actions that they considered to be "push" and "stroke" operations. The order of operations for each operator was determined by a standard Latin square design, i.e., a different order for operators, to eliminate any order effects.

3.2 Feature values of finger operations

Quantitative analysis was performed to determine feature descriptors that are better able to classify push and stroke operation with haptic feedback. Type A objects, i.e., three types of low-resilience urethane with different thickness, as shown in Fig. 3, were selected as the operation targets. To investigate the classification performance of these feature values, we first focused on characteristics of the 2D feature sets: one chosen from normalized strain and the other from velocity.

Figure 5a shows the 2D plot of the typical feature sets (v_a, ϵ_a), (v_σ, ϵ_a), (v_a, ϵ_σ), and $(v_\sigma, \epsilon_\sigma)$ calculated from the measured data using $w = 30$. Figure 5b shows the 2D plot of feature set (v_σ, ϵ_a) for each w value. Parameter w, which is the width of the window that evaluates the time-series measured data, was set to 40, 30, 20, and 10. The differences in the number of feature value plots according to the value of w are due to the differences in contact detection. Window widths w = 40, 30, 20 and 10 required 1.2, 0.9, 0.6 and 0.3 s, respectively, to detect contact because a contact state was identified when $\epsilon(t) > \epsilon_0$ were satisfied for all $\epsilon(t)$ within the window. Therefore, smaller w values result in larger sampled feature sets. As each feature value is determined by fewer measurement values over a short period of time, the feature values become sensitive to finger operation. In contrast, as w increases, more sampled data are used for contact detection, and the number of feature values extracted from the measured data of each subject decreases. We can confirm these characteristics of sampled feature values in Fig 5b.

Table 1 shows the recognition rates of the four feature

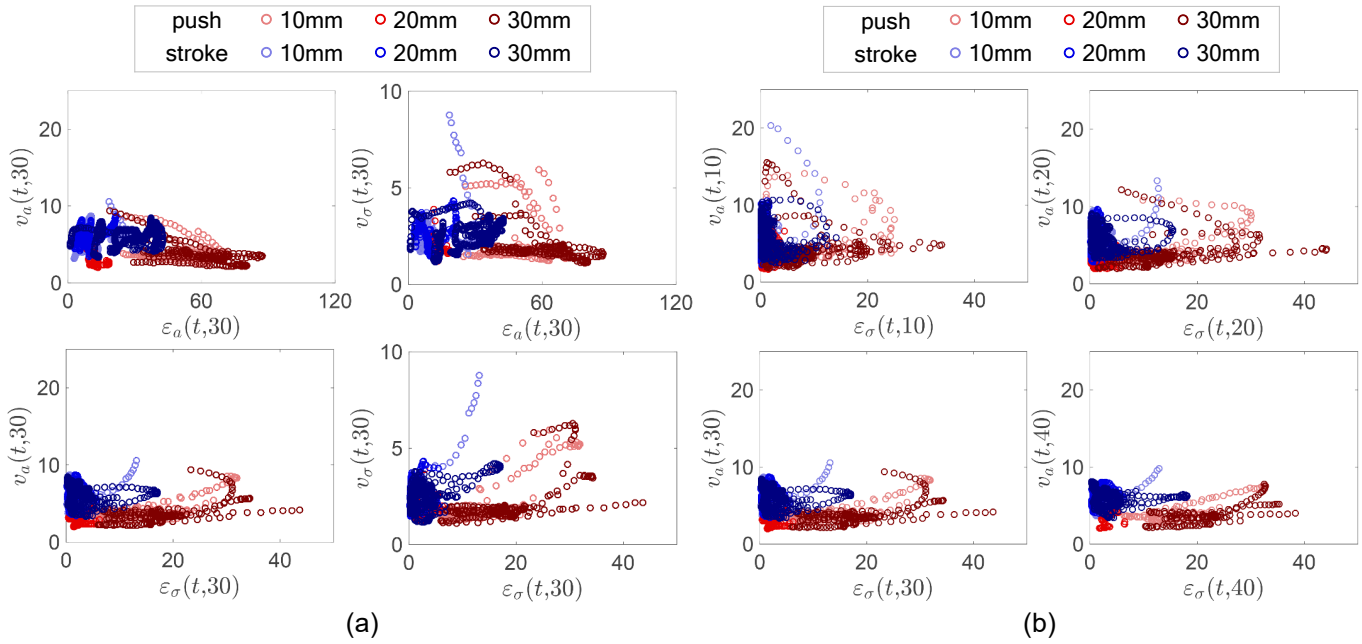

Fig. 5. Examples of feature value distribution on normalized strain and velocity in push and stroke manipulations: (a) 2D plot of different feature sets with time window width $w = 30$ and (b) 2D plot of feature set (v_σ, ϵ_a) with different time window widths.

values for each of the four w values. The classification results were computed by binary classification using an SVM and 10-fold cross validation for each subject. The ten datasets were divided into nine training datasets and one test dataset. The decision boundary was computed from the nine training datasets, and then applied to the test dataset. The same procedure was conducted for all (ten) patterns of training/test datasets while changing the test dataset. This validation can determine cross-subject recognition rates for all subjects, and all patterns of test data were equivalently analyzed. The highest push and stroke operation detection rate was obtained when using $v_a(t,w)$ and $\varepsilon_\sigma(t,w)$. In terms of recognition rate for each subject, the lowest recognition rate ($w = 10 : 69.37\%$, $w = 20 : 73.95\%$, $w = 30 : 77.66\%$, and $w = 40 : 80.07\%$) was obtained when the feature set (v_a, ε_σ) was used as test data. When using other feature value sets, the recognition rates were even lower. Therefore, the combination of $v_a(t,w)$ and $\varepsilon_\sigma(t,w)$ was considered to be the most suitable for classifying push and stroke operations.

We next determined the optimal w value for classifying push and stroke operations. When $v_a(t,w)$ and $\varepsilon_\sigma(t,w)$ were treated as feature values, smaller w values decreased the recognition rate. In contrast, smaller w leads to a finger operation classification system with higher sensitivity and short computation time. We hypothesized that a human's push and stroke operations can be classified by low-dimensional features of the fingerpad information. Although achieving a higher recognition rate is desirable, maximizing the recognition rate and the minimizing the time frame for evaluation is a trade-off. Because the experiments showed one motion for a push or stroke operation ranges from 1 to 3 s, $w = 30$ was considered to be a good value for recognizing finger operations. The detection rate was greater than 90% when $w = 40$ (91.16%) and $w = 30$ (90.34%), which are both acceptable values for classifying operations. Thus, the 2D feature set $v_a(t,w)$ and $\varepsilon_\sigma(t,w)$ with window width $w = 30$ should perform well and be suitable for finger operation analysis.

TABLE 1
Recognition rates for different combinations of feature sets and time window parameters.

	$w = 40$	$w = 30$	$w = 20$	$w = 10$
(ϵ_a, v_a)	86.64	86.90	83.90	77.88
(ϵ_a, v_σ)	69.21	71.58	72.08	68.39
(ϵ_σ, v_a)	91.16	90.34	88.10	83.14
$(\epsilon_\sigma, v_\sigma)$	79.38	81.03	80.65	77.44

3.3 Robustness of feature values

The goal of the analysis in this experiment was to investigate the classification accuracy of the push and stroke operations for multiple elastic bodies of different thicknesses, stiffnesses, and shapes. We analyzed the finger operation measurement values for 10 subjects on nine types of elastic bodies, as shown in Fig. 3. Type B objects were cuboids (22-mm-thick) constructed from low-resilience urethane, gel (soft) and gel (hard), i.e., only the stiffness varied. To reduce differences in the sense of touch on the surface due to the materials, type B objects were covered in a wrap during the finger operation measurement. Type C objects had different shapes, i.e., cuboid, hemispheric, and triangular. All type C objects were constructed from soft gel.

To examine the robustness of the feature set (v_a, ϵ_σ), with $w = 30$ as selected by the previous experiments, the next experiments confirmed the recognition rates for all fifteen combinations of feature sets (F1–F15) defined by 4D features $(v_a, v_\sigma, \epsilon_a, \epsilon_\sigma)$ were considered. The naming convention for

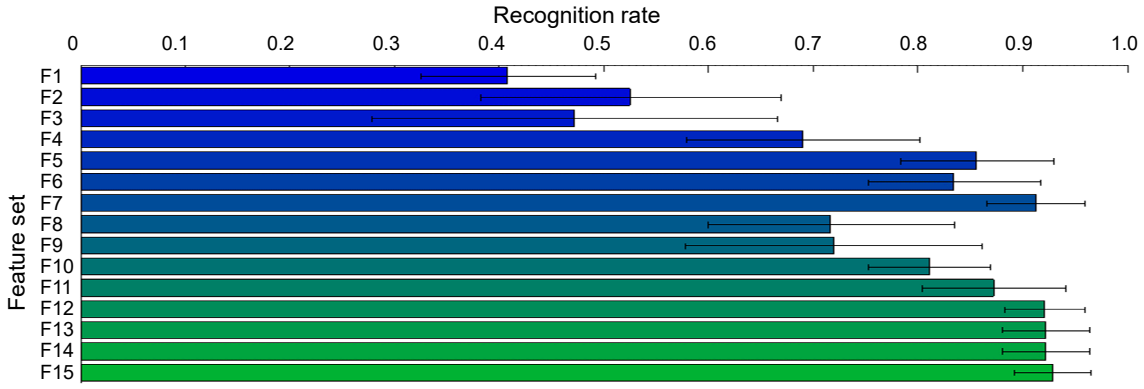

Fig. 6. Comparison of classification performance. Two-dimensional feature sets using velocity and strain values outperformed 1D features. Specifically, F7 shows the best performance in the 2D feature group, and a significant difference was found between F7 and the other 2D features. Furthermore, F12, F13, F14, and F15 also achieve recognition rates of more than 90%. However, there are no significant differences between F7 and these higher dimensional features. These results suggest that the combination of velocity and strain values is a good feature descriptor for classifying push and stroke operations.

the feature sets is given in Table 2. Similar to the previous analysis, the recognition rate was calculated from the measured data on all nine elastic objects for each subject. This experimental setting also provides comparative results between the performance of the proposed multidimensional features and that of other recognition approach with a 1D feature. In this experiment, 90% was used as the target recognition rate.

TABLE 2
Naming convention for multidimensional feature sets.

dimension	name	feature sets
1D feature	F1	(v_a)
	F2	(ϵ_a)
	F3	(v_σ)
	F4	(ϵ_σ)
2D features	F5	(v_a, ϵ_a)
	F6	(v_a, v_σ)
	F7	(v_a, ϵ_σ)
	F8	(ϵ_a, v_σ)
	F9	$(\epsilon_a, \epsilon_\sigma)$
	F10	$(v_\sigma, \epsilon_\sigma)$
3D features	F11	$(v_a, \epsilon_a, v_\sigma)$
	F12	$(v_a, \epsilon_a, \epsilon_\sigma)$
	F13	$(v_a, v_\sigma, \epsilon_\sigma)$
	F14	$(\epsilon_a, v_\sigma, \epsilon_\sigma)$
4D features	F15	$(v_a, v_\sigma, \epsilon_a, \epsilon_\sigma)$

Figure 6 shows the classification results obtained using SVM learning and 10-fold cross validation. The average recognition rate of 1D features were around 50% chance level, which mean a single feature of velocity or strain fails to discriminate push and stroke operations. The average recognition rates of 2D feature sets outperformed the 1D features. Specifically, the combination of the velocity and strain values achieve better performance. Specifically, F7 shows the best performance in the 2D feature group. Significant differences were found between F7 and 1D features by one-way analysis of variance (ANOVA, $p < 0.05$ significance level): F1 (F(1,18)=250.9), F2 (F(1,18)=59.3), F3 (F(1,18)=43.9), and F4 (F(1,18)=30.4). Significant differences were also found between F7 and 2D features: F6 (F(1,18)=6.1), F8 (F(1,18)=21.3), F9 (F(1,18)=15.1), and F10 (F(1,18)=16.5). Regarding higher dimensional feature sets, F12, F13, F14, and F15 also achieved a recognition rate of more than 90%. However, the average recognition rate is still around 90%, and there are no significant differences between F7 and these feature sets. These comparison results suggest that the combination of velocity and strain values is a good feature descriptor for classifying push and stroke operations.

The recognition rate calculated from cross validation of the classification results for each subject is shown in Fig. 7a. An average recognition rate of 91.2% was obtained, which is higher than the detection rate for the previous analysis using SVM learning with type A objects only (90.3%). Furthermore, in terms of the recognition rate for each subject, we can confirm, with an accuracy rate of 80% or more for each subject, that the operation classification was stably successful. Figure 7b shows the accuracy rate with the respective measurement values for the nine elastic bodies. The labels on the x-axis of the figure are the ID numbers assigned to the elastic bodies shown in Fig. 3. The average recognition rate was 91.4%. As the recognition rate for each operation target was 80% or more, we can confirm that it robustly classified push and stroke operations.

4 Discussion

It is not easy to quantitatively analyze the tactile information obtained by humans when they directly touch an object. The proposed measurement system addresses this issue and enables simultaneous measurement of finger position and fingertip strain without inhibiting the sense of touch. In this context, this study is the first attempt to perform a quantitative analysis based on the tactile information of natural finger operations. We focused on the quantitative classification of single-finger push and stroke operations, and found that the 2D features of fingertip position $\mathbf{p}(t)$ and strain $\epsilon(t)$ with a 0.9-s time frame ($w = 30$) could achieve good classification performance. Figs. 7 and 8 show that using $v_a(t, 30)$, $\epsilon_\sigma(t, 30)$, even with push and stroke operations on elastic bodies of different forms, stiffnesses,

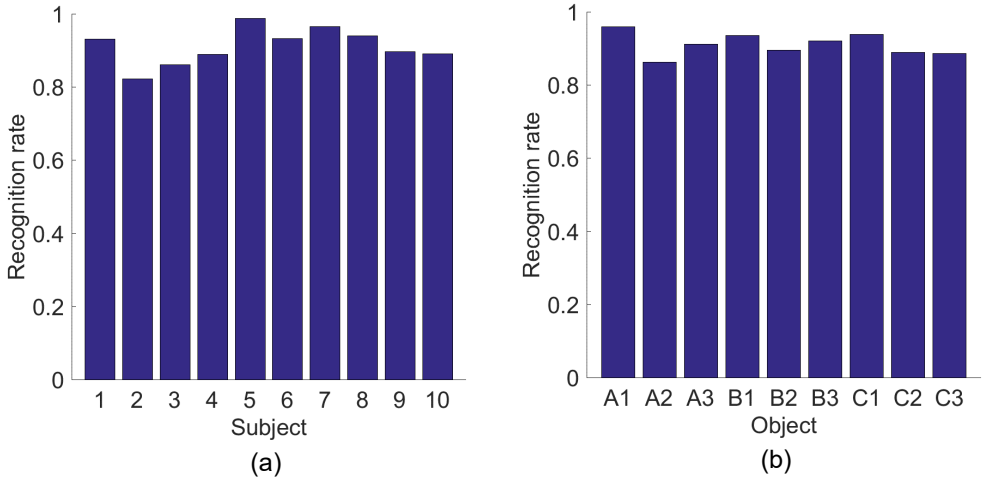

Fig. 7. Classification performance of feature set F7: (a) recognition rates for different subjects and (b) recognition rates for different operation targets.

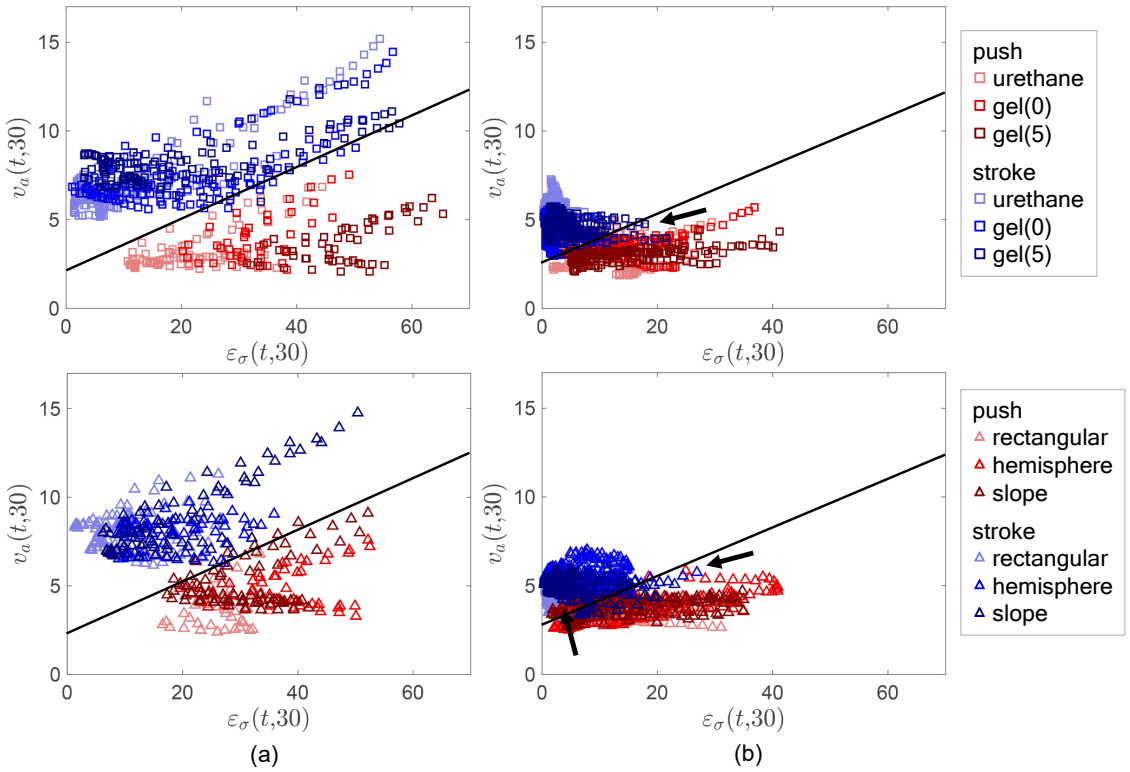

Fig. 8. Decision boundary obtained from SVM learning: data for (a) operator 1 and (b) operator 2. Regardless of the stiffness and shape of the target elastic objects, the feature set can classify push and stroke operation with small recognition errors.

and thicknesses, classification can be achieved with a high recognition rate. The recognition rate (91.20%) for the nine types of elastic objects was higher than that for type A objects (90.34%). As the number of elastic bodies targeted for operation increased, the number of data used as training data increased. This demonstrates that the increase in amount of training data improved the reliability of the calculated linear decision boundaries.

Feature set $v_a(t,30)$ and $\epsilon_\sigma(t,30)$ for operator 1 is plotted in Fig. 8a. In the figure, different markers are assigned to the feature values obtained from different types of elastic objects. The figure shows that irrespective of the stiffness and shape of the target object, the feature values for the push and stroke operations form a cluster concentrated within a certain area. It also demonstrates that a linear decision boundary can classify the data into two categories with low classification error. Fig. 8b shows another 2D plot of $v_a(t,30)$, and $\epsilon_\sigma(t,30)$ for operator 2. We chose these two examples because they showed remarkable differences from the viewpoint of operations. The feature data of operator 1 are widely distributed for both push and stroke operations; thus, we can confirm that the finger operations

are significantly different. Operator 1 pushes with a large motion and operator 2 pushes with relatively small motion. Regardless of the stiffness and shape of the target elastic objects, the feature values for the push and stroke operations form clusters similar to those of operator 1. Figure 7a shows that the recognition rate for operator 2 was lowest. The several plots indicated by the three arrows in Figure 8b are misclassified results. Actually, the motion of operator 2 was the smallest of the subjects. This suggests a natural fact that it is more difficult to identify smaller motions, and this is considered to be a limitation of the proposed recognition framework. Another possible reason for the recognition errors may come from the elasticity of the fingerpad. The relationship between fingerpad stiffness and recognition rate is an interesting topic. The exploration of a nonlinear decision boundary to improve the classification performance is also an important topic for further study.

Regarding the limitations of this study, it concentrated on a quantitative analysis of only simple push and stroke operations using a single finger. The evaluated shapes and material properties are also a limitation of this experiment. As the elastic test objects required high reproducibility, we prepared six types of elastic objects with different shapes and stiffness as a first trial for finger operation recognition. To show the sufficiency of the selected feature values requires additional object variations. More complex finger operations and objects should reduce the recognition rate. On the contrary, through closer scrutiny of the feature values extracted from the finger operation measurement values, an increase in the amount of training data from more measurement values is expected to lead to a broader range of detectable finger operations.

Quantitatively classifying natural human finger operations is expected to lead to applications in various fields. For example, it is expected that this will lead to an essential understanding of dexterous finger operations using sense of touch. The findings may be also useful for diagnosis of finger operations with haptic feedback [29] and the design of autonomous robotics manipulators capable of performing actions similar to human finger operations [11], [12]. Furthermore, it is also considered a valid novel interface for applications that use finger operations on actual objects as input [30], [37], [40]. More specifically, it is possible that quantitative information from finger operations could replace touch interfaces. For instance, by using the fact that the push/stroke performed by the user can be discriminated based on the deformation and speed of the fingertip, it is possible to have various shapes and materials such as rubber and cloth without restricting operation to current dedicated touch screens. Touch on any real object can be the input for a computer using HapLog-like wearable devices. Based on these contexts and further applications, we believe that analyzing common fingertip features not dependent on the shape and material of the object will be an interesting topic. Future work is necessary to investigate more complex, dexterous operations with multiple fingers. We believe that the developed measurement system design and experimental procedures can be applied to a systematic understanding of specialized human operations.

5 Conclusion

To quantitatively understand natural finger operations used to manipulate elastic objects, this study explored low-dimensional robust feature descriptors that are invariant to operator, finger position, and target object. We developed a wearable system that enables the simultaneous measurement of fingertip position and strain without inhibiting the operator's sense of touch. User experiments were designed to obtain time-series fingertip position and strain from 10 subjects touching nine types of elastic objects, and the quantitative classification of the push and stroke operations of a single finger was investigated. The results show that the two-dimensional features obtained from fingertip position and strain within a 0.9-s time frame can stably recognize push and stroke operations on elastic bodies of different shapes, stiffnesses, and thicknesses at a higher recognition rate.

Acknowledgments

This research was supported by JSPS Grant-in-Aid for Scientific Research (B) (15H03032).

References

[1] . G.C. Burdea, *Force and touch feedback for virtual reality*, John Wiley & Sons, Inc., 1996.
[2] M. O. Ernst and M.S. Banks, "Humans integrate visual and haptic information in a statistically optimal fashion," *Nature*, vol. 415, pp. 429–433, 2002.
[3] A. Moscatelli, V. Hayward, M. Wexler and M. O. Ernst, "Illusory tactile motion perception: An analog of the visual Filehne illusion," *Scientific Reports*, vol. 5, 14584, 2015.
[4] J. Platkiewicz, H. Lipson and V. Hayward, "Haptic edge detection through shear," *Scientific Reports*, vol. 6, 23551, 2016.
[5] W.J. Adams, I.S. Kerrigan, and E.W. Graf, "Touch influences perceived gloss," *Scientific Reports*, vol. 6, pp. 21866, 2016.
[6] M. Nakao, T. Kuroda, M. Komori and H. Oyama, "Evaluation and user study of haptic simulator for learning palpation in cardiovascular surgery," *International Conference of Artificial Reality and Tele-Existence (ICAT)*, pp. 203–208, 2003.
[7] M. Nakao, T. Kuroda, M. Komori, H. Oyama, K. Minato and T. Takahashi, "Transferring bioelasticity knowledge through haptic interaction," *IEEE MultiMedia*, vol. 13, no. 3, pp. 50–60, 2006.
[8] J.N. Howell et al., "The virtual haptic back: a simulation for training in palpatory diagnosis," *BMC Med. Educ.*, vol. 8, no. 14, 2008.
[9] T. R. Coles, D. Meglan and N. John, "The role of haptics in medical training simulators: A survey of the state of the art," *IEEE Trans. on Haptics*, vol. 4, pp. 51–66, 2011.
[10] V. Duchaine and C.M. Gosselin, "General model of human-robot cooperation using a novel velocity based variable impedance control," *Proc. World Haptics*, pp. 446–451, 2007.
[11] D. R. Faria, R. Martins, J. Lobo and J. Dias, "Extracting data from human manipulation of objects towards improving autonomous robotic grasping," *Robotics and Autonomous Systems*, vol. 60, pp. 396–410, 2012.
[12] U. Prieur, V. Perdereau, and A. Bernardino, "Modeling and planning high-level in-hand manipulation actions from human knowledge and active learning from demonstration," *IEEE/RSJ International Conference on Intelligent Robots and Systems (IROS)*, pp. 1330–1336, 2012.
[13] K.A. Nichols and A.M. Okamura, "Autonomous robotic palpation: Machine learning techniques to identify hard inclusions in soft tissues," *IEEE International Conference on Robotics and Automation (ICRA)*, pp. 4384–4389, 2013.
[14] I. M. Bullock, R. R. Ma and A. M. Dollar, "A hand-centric classification of human and robot dexterous manipulation," *IEEE Tran. on Haptics*, vol. 6 no. 2, pp. 129–144, 2013.
[15] H. Soh and Y. Demiris, "Incrementally learning objects by touch: Online discriminative and generative models for tactile-based recognition," *IEEE Trans. on Haptics*, vol. 7, pp. 512–25, 2014.

[16] M.M. Rahman, R. Ikeura, and K. Mizutani, "Control characteristics of two humans in cooperative task and its application to robot control," *26th Annual Conference of the IEEE Industrial Electronics Society*, vol. 3, pp. 1773–1778, 2000.
[17] S. Whittaker, S. Tucker, K. Swampillai and R. Laban, "Design and evaluation of systems to support interaction capture and retrieval," *Personal and Ubiquitous Computing*, vol. 12, pp. 197–221, 2008.
[18] M. Li, A. Faragasso, J. Konstantinova et al., "A novel tumor localization method using haptic palpation based on soft tissue probing data," *IEEE International Conference on Robotics and Automation (ICRA)*, pp.4188–4193, 2014.
[19] R.H. Cuijpers, J.B. Smeets and E. Brenner, "On the relation between object shape and grasping kinematics," *J Neurophysiol.*, vol. 91, pp. 2598–606, 2004.
[20] J. Rosell, R. Surez, C. Rosales and A. Prez "Autonomous motion planning of a hand-arm robotic system based on captured human-like hand postures," *Autonomous Robots*, vol. 31, pp. 87–102, 2011.
[21] P. Sandilands, M.G. Choi and T. Komura, "Interaction capture using magnetic sensors," *Computer Animation and Virtual Worlds*, vol. 24, pp. 527–538, 2013.
[22] T. Feix, I.M. Bullock and A.M. Dollar, "Analysis of human grasping behavior: Object characteristics and grasp type," *IEEE Trans Haptics*, vol. 7, no. 3, pp. 311–23, 2014.
[23] F. E. Beek, W. M. B. Tiest, W. Mugge and A. M. L. Kappers, "Haptic perception of force magnitude and its relation to postural arm dynamics in 3D," *Scientific Reports*, vol. 5, 18004, 2015.
[24] C. E. Madan, A. Kucukyilmaz, T. M. Sezgin and C. Basdogan, "Recognition of haptic interaction patterns in dyadic joint object manipulation," *IEEE Trans. on Haptics*, vol. 8, no. 1, pp. 54–66, 2015.
[25] D. Wang, Y. Zhang and C. Yao, "Stroke-based modeling and haptic skill display for Chinese calligraphy simulation system," *Virtual Real.*, vol. 9, pp. 118–132, 2006.
[26] Y. Ishibashi and T. Asato, Media Synchronization Control with Prediction in a Remote Haptic Calligraphy System, *Proc. ACM SIGCHI*, pp. 79-86, 2007.
[27] Y. Kuroda, M. Hirai, M. Nakao, T. Sato, T. Kuroda, K. Nagase and H.Yoshihara "Organ exclusion simulation with multi-finger haptic interaction for open surgery simulator," *Stud. Health Technol. Inform.*, vol. 125, pp. 244–249, 2007.
[28] M. J. Rissanen, Y. Kuroda, N. Kume, M. Nakao, T. Kuroda, H. Yoshihara, "Audiovisual guidance for simulated one point force exertion tasks," *Proc. VRCIA'06*, pp. 365-368, 2006.
[29] D. Austin, J. McNames, K. Klein, H. Jimison and M. Pavel. "A statistical characterization of the finger tapping test: Modeling, estimation, and applications," *IEEE Journal of Biomedical and Health Informatics*, vol. 19, no. 2, pp. 501–507, 2015.
[30] F. Wang, X. Cao, X. Ren and P. Irani, "Detecting and leveraging finger orientation for interaction with direct-touch surfaces," *Proc. of UIST'09*, pp.23-32, 2009.
[31] S. A. Mascaro and H. H. Asada, "Photoplethysmograph fingernail sensors for measuring finger forces without haptic obstruction," *IEEE Transactions on Robotics and Automation*, vol. 17, pp. 698–708, 2001.
[32] R. Kikuuwe and T. Yoshikawa, "Haptic display device with fingertip presser for motion/force teaching to human," *IEEE International Conference on Robotics and Automation(ICRA)*, vol. 1, 868–873, 2001.
[33] P.G. Kry and D.K. Pai, "Interaction capture and synthesis," *ACM Trans. Graph.* vol. 25, pp. 872–880, 2006.
[34] M. Nakao, R. Kitamura, T. Sato and K. Minato, "A model for sharing haptic interaction," *IEEE Trans. on Haptics*, vol. 3, no. 4, pp. 292–296, 2010.
[35] F. Ohno, M. Nakao and T. Matsuda, "Finger force and position measurement without obstructing touch interaction," *Proc. Annual International Conference of the IEEE Engineering in Medicine and Biology Society (EMBC)*, U-7, 2013.
[36] S.J. Lederman and K.L. Roberta, "Hand movements: A window into haptic object recognition," *Cognitive psychology*, vol. 19 no. 3, pp. 342–368, 1987.
[37] D. Holman and R. Vertegaal, "Organic user interfaces:Designing computes in any way, shape, or form," *Communication of the ACM*, vol. 51, pp. 48–55, 2008.
[38] C. Harrison, H. Benko and A. D. Willson, "OmniTouch: Wearable multitouch interaction everywhere," *Proc. of UIST'11*, pp. 441–450, 2011.
[39] Y. Makino, M. Murao and T. Maeno, "Life log system based on tactile sound," *EuroHaptics* vol. 1, pp. 292–297, 2010.
[40] C. Stewart, M. Rohs, S. Kratz and G. Essl, "Characteristics of pressure-based input for mobile devices," *Proc. CHI '10*, pp. 801-810, 2010.
[41] Ring, Logbar Inc., "http://logbar.jp/ring/en."
[42] M. Nakatani, T. Kawasoe, K. Shiojima, K. Koketsu, S. Kinoshita and J. Wada, "Wearable contact force sensor system based on fingerpad deformation," *Proc. World Haptics*, pp. 323–328, 2011.

Megumi Nakao received the Ph.D. degree in informatics from Kyoto University, Kyoto, Japan, in 2003. After working at Graduate School of Medicine, Kyoto University and Graduate School of Information Science, Nara Institute of Science and Technology, Nara, Japan, he is currently the associate professor in Biomedical Engineering Lab. at Graduate School of Informatics, Kyoto University, Kyoto, Japan. His research interests include biomedical engineering, machine intelligence in biomedicine and virtual reality.

Masayuki Senoo received the M.S. degree in informatics from Kyoto University, Kyoto, Japan, in 2016. He is currently working at Technology Planning Department, General Technology Division, Central Japan Railway Company, JAPAN.

Tetsuya Matsuda received the M.D. degree from Faculty of Medicine, Kyoto University, Kyoto in 1981 and received the Ph.D. degree from Graduate School of Medicine, Kyoto University in 1988. After working at Third Division, Department of Internal Medicine, Kyoto University Hospital, Division of Cardiovascular Disease, University of Alabama at Birmingham, and Department of Medical Informatics, Kyoto University Hospital, he serves as Professor, Department of Systems Sciences, Graduate School of Informatics, Kyoto University from 2000. His research field covers magnetic resonance imaging, medical image processing and cardiac simulation.